View Article Online
View Journal

Green Chemistry

Cutting-edge research for a greener sustainable future

Accepted Manuscript

This article can be cited before page numbers have been issued, to do this please use: S. Mazzotta, M. Piro, E. Cassera, M. Gerola, M. Fagnoni, D. Ravelli and A. Bernardi, *Green Chem.*, 2026, DOI: 10.1039/D5GC05775B.

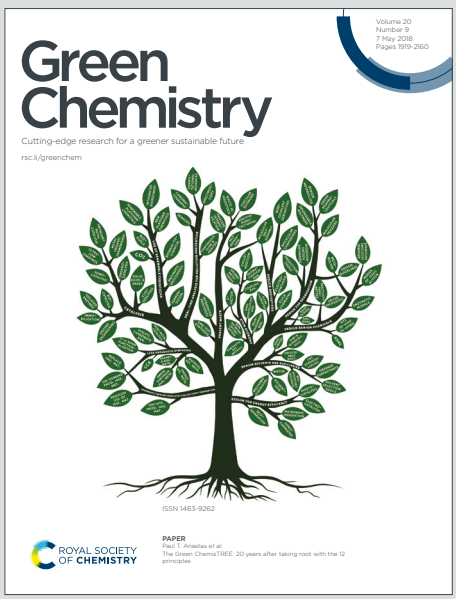

Green foundation

View Article Online
DOI: 10.1039/D5GC05775B

1. The present work developed a sustainable photocatalytic approach for the preparation of C-5 alkylated fucosides directly from the corresponding β-fucosides, with no need of pre-activation of the starting glucosides.

2. Beside providing an unprecedented transformation of the pyranose core, this approach represents a 100% atom economy process that avoids the use of any additives via site-selective C-H cleavage in β-fucosides by adopting an easily prepared photocatalyst.

3. Future research will focus on applying this sustainable strategy for the late-stage functionalization of further glucosides.

View Article Online
DOI: 10.1039/D5GC05775B

ARTICLE

Editing Sugars: Decatungstate Photocatalyzed Site- and Stereoselective C-H Functionalization in β-Fucosides

Received 00th January 20xx,
Accepted 00th January 20xx

DOI: 10.1039/x0xx00000x

Sarah Mazzotta,*[a] Matteo Piro, [a] Elena Cassera, [b] Michele Gerola, [a] Maurizio Fagnoni, *[b] Davide Ravelli, [b] Anna Bernardi *[a]

C–H Bond functionalization via (photoinduced) Hydrogen Atom Transfer (HAT) catalysis is emerging as a powerful eco-sustainable tool for sugar editing, albeit challenges in governing the reactivity patterns and site-selectivity remain. Quite surprisingly, no functionalization of the C-5 position in pyranoses via C–H activation has been described to date. We herein report the development of an efficient methodology for the site-selective and stereoselective alkylation of position 5 of β-fucosides by means of decatungstate photocatalyzed C(sp^3)–C(sp^3) bond formation. The experimental work is accompanied by spectroscopical studies based on laser flash photolysis and supplemented by computational simulations, offering insights into the reasons underlying the selectivity profile of the reported transformations.

Introduction

Chemical modification of carbohydrates plays a significant role in materials science, biotechnology, as well as in drug design and development. As for the latter field, sugars elaboration allows to enhance drug activity, stability, and specificity, and is key in studying molecular recognition events and developing targeted therapies like antibody-drug conjugates.[1] However, modifying sugars is challenging due to their complex structure and reactivity, associated with chemo-, regio- and stereo-selectivity issues. In the case of pyranose derivatives, the modification may take place at carbons C-1 – C-5 in the ring or at the exocyclic C-6 position (Figure 1 A) where metal-catalysis can be helpful in this respect.[2–4]. The manipulation of sugars typically occurs by substitution at the anomeric position, where the high reactivity of the hemiacetal functionality enables selective modifications.[5,6] The strategy forces the preactivation of the anomeric carbon by the presence of appropriate leaving groups.[7] Photoinduced glycosylation via glycosyl radicals (Figure 1 B) has attracted increasing interest in recent years, due to the compatibility of such intermediates with a wide range of functional groups and thanks to the mild conditions required for promoting the process. Typically, the strategy foresees the installation of a redox active moiety at the anomeric position, which is then lost in the photocatalytic event.[7–13]

The modification of carbohydrates' skeleton at a non-anomeric position is traditionally achieved by functional group manipulation of the native hydroxy groups.[14] However, direct C–H bond functionalization is currently emerging as a powerful and sustainable tool for sugar editing, including the non-enzymatic synthesis of rare carbohydrates, many of which are contained in naturally occurring antibiotics and other drugs.[15–19] Especially in the context of glycomimetic design, modifications of monosaccharides' skeleton via C–H activation can be transformative, because they enable functionalization of the sugar scaffold while preserving the crucial hydroxyl groups pattern for target recognition.[20,21]

However, while C–H functionalization methodologies do not need any pre-activation of substrates and thus decrease the number of synthetic steps, they can be extremely challenging in terms of reactivity and site-selectivity; therefore, despite the huge synthetic potential, such approaches are still underdeveloped for the functionalization of carbohydrates.

Photocatalyzed hydrogen atom transfer (HAT) reactions represent a valuable eco-sustainable tool to perform a clean C–H homolytic cleavage, even in complex substrates, for the generation of C-based radicals.[22] As a matter of fact, this approach has been recently applied for the C–H functionalization of both protected and unprotected monosaccharides. The resulting scenario is quite complex to

[a] Dipartimento di Chimica, Università degli Studi di Milano, Via C. Golgi, 19 – 20133 Milano, Italy.
[b] PhotoGreen Lab, Department of Chemistry, University of Pavia, Viale Taramelli 12, 27100 Pavia, Italy.

Supplementary Information available: Experimental procedures, characterization data of synthesized compounds, details of additional experiments, LFP data, DFT analysis, NMR spectra (PDF). See DOI: 10.1039/x0xx00000x

View Article Online
DOI: 10.1039/D5GC05775B

summarize, since hydrogen abstraction depends on several factors, that include: the nature and the bulkiness of the hydrogen abstracting agent, the structure of the monosaccharides as well as the steric hindrance (or the electronic effects) exerted by the presence of protecting groups and the presence of additives (e.g. Brønsted base co-catalysts).[15–19]

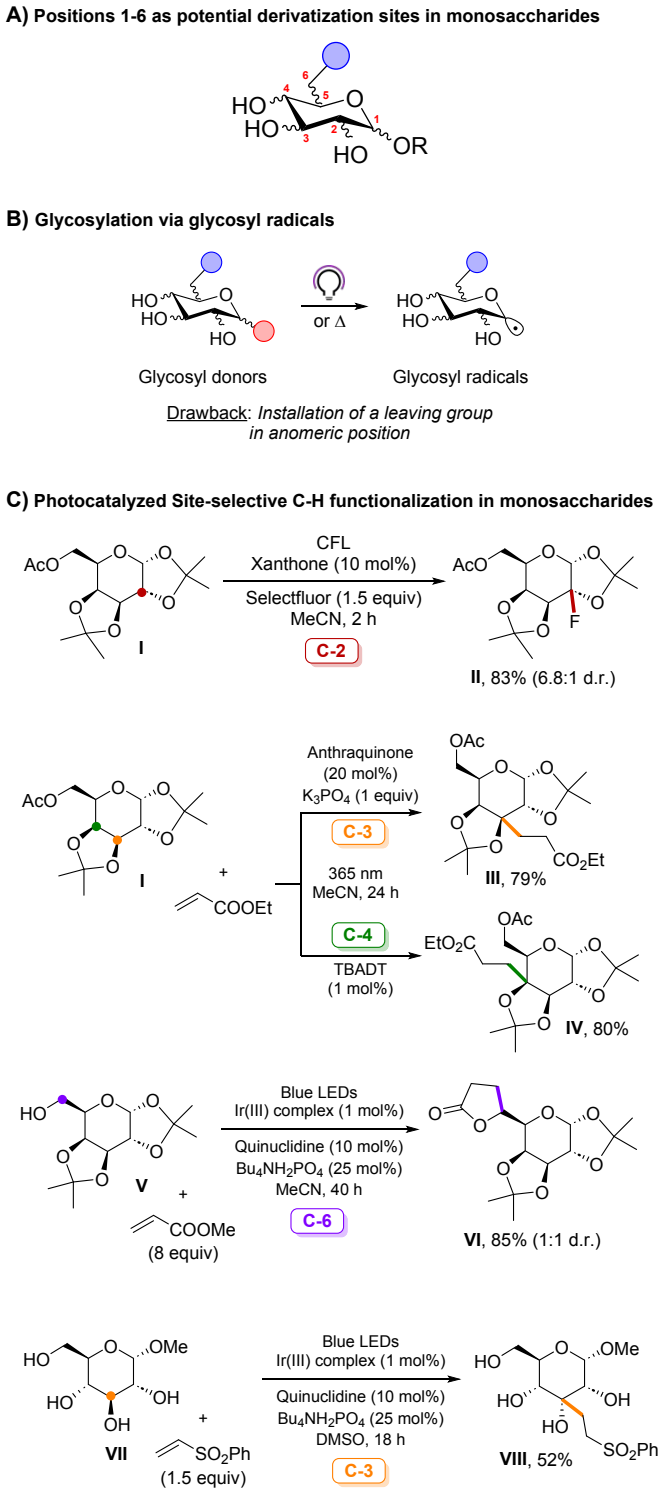

Fig. 1 Derivatization of monosaccharides: **A)** Potential derivatization sites. **B)** Typical strategy for the generation of glycosyl radical and ensuing derivatization at C-1. **C)** Selected photocatalytic systems for the site-selective C–H elaboration in different positions.

Figure 1c illustrates selected examples to clarify this issue. First, protected galactopyranose **I** was fluorinated at C-2 to deliver product **II** by direct HAT employing an aromatic ketone (xanthone) as the photocatalyst (PC).[23] Noteworthy, when changing PC, the selectivity in the hydrogen abstraction on the same derivative **I** dramatically changed. A C-3 selectivity was exclusively observed by using anthraquinone,[24,25] whereas a completely selective C-4 functionalization took place when adopting the decatungstate anion, either as tetrabutylammonium (TBADT; for C–C bond formation)[24] or sodium (NaDT; for fluorination)[25] salt. Overall, such strategies offered straightforward access to Giese adducts **III** and **IV** in a good yield.[24] Similarly, the photocatalytically generated quinuclidine radical cation operated a HAT on 6-deacetylated galactose derivative **V** leading to the side chain modification at C-6 (delivering lactone **VI**).[26] The same reaction conditions applied to derivative **VII** (α-methyl glucoside) restored the derivatization at C-3 (on the route to **VIII**).[27] These examples confirm the intricacies related to predicting the fate of the C–H functionalization on carbohydrates.[28–30] Nevertheless, the study of the factors that lower the bond dissociation energy and decrease the kinetic barrier for hydrogen atom abstraction allowed for a radical-mediated site-selective epimerization of unprotected monosaccharides by HAT,[19,31–33] where the concept of network control has been proposed to account for the observed selectivity.[34] As apparent from Figure 1, the C-1[35,36] and C-5 positions are the most challenging to modify via direct C–H functionalization, even if the C–H elaboration at the anomeric position of C-glycosides via radical bromination (typically with NBS) has long been known.[37,38]

Molecular editing at the C-5 position of pyranoses is of particular significance, as this position is often involved in enzyme-substrate interactions[39] and in molecular recognition of carbohydrate-binding proteins. This transformation could expand the chemical space available for carbohydrate-based drugs[40] by adding functional groups to the carbohydrate skeleton. During our research program on the fucose-specific bacterial lectin BC2L-C,[41–44] for instance, we became interested in modifying the position 5 of β-fucosides, to simultaneously reach sterically divergent secondary sites of the protein. L-fucose is a component of blood group antigens, glycoproteins, and glycolipids involved in cell communication and pathogen recognition. On the other hand, the D-enantiomer is usually found in plants and in some microorganisms.[45] Accordingly, modifying fucose at C-5 is key to expanding the chemical space for inhibitors and probes targeting these biological processes.

A literature survey indicates that the photocatalyzed C–H manipulation in 6-deoxy-monosaccharides, such as fucopyranosides (**XI**) or rhamnopyranosides (**IX**, **XIII**) is quite rare (Figure 2). In such cases, a Ph_2BOH co-catalyst was adopted to direct selectivity.[46] It is impressive to note that the photocatalyzed reaction between methyl α-L-rhamnopyranoside **IX** and methyl acrylate gave lactone **X** via exclusive C–H elaboration at C-2 (Figure 2a). On the contrary, the site-selectivity diverted when the same reaction conditions were applied to methyl α-L-fucopyranoside **XI**, wherein a C-4/C-3 = 5.3:1 mixture of adducts **XII** resulted (Figure 2b). Moreover, in the attempt of obtaining valuable 5-C-bromosugars, a radical C-5 bromination on

View Article Online
DOI: 10.1039/D5GC05775B

methyl tetra-O-acetyl-α-L-rhamnopyranoside **XIII** dramatically failed (Figure 2c).[47]

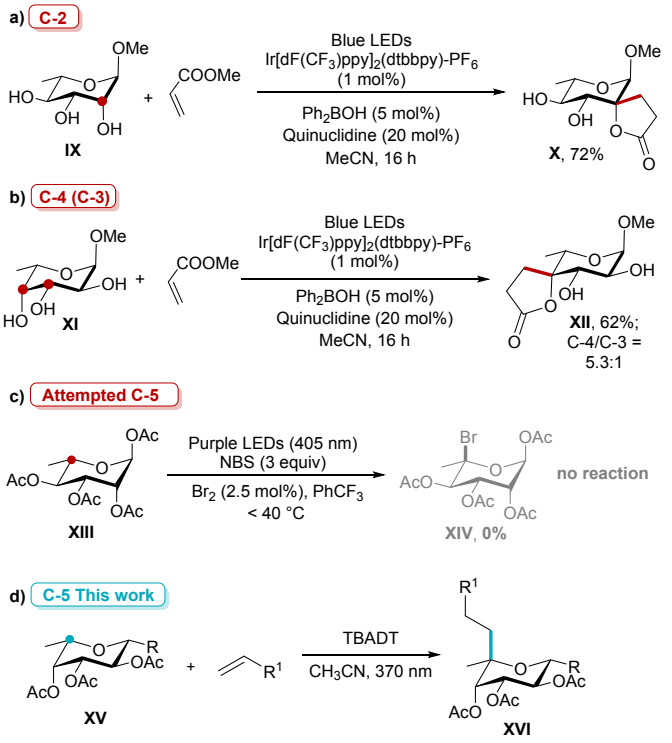

Fig. 2 Photoinduced C–H elaboration in: **a)** rhamnopyranosides or **b)** fucopyranosides. **c)** Attempted bromination at C-5 in rhamnopyranosides. **d) This work**: functionalization at C-5 in fucopyranosides.

We then realized that, to the best of our knowledge, the direct C–H functionalization at position 5 of monosaccharides is still lacking. Based on our experience on TBADT photocatalysis,[48,49] we envisaged that this easily prepared photocatalyst could be useful for such purpose, provided that the right protecting groups/substituents are present in the starting fucopyranoside. Herein, we report the development of an efficient methodology for the selective alkylation of position 5 of fucose by a TBADT photo-mediated Giese type alkylation (Figure 2d).

Results

Preparative Experiments. To achieve C-5 editing of β-fucosides, we reasoned that protection of the starting pyranoside as a β-tetra-acetate (Figure 2d; **XV**, R = OAc) could be an interesting starting point on different grounds. First, we surmised that a β-OAc group in the anomeric position would not sterically hinder C-5 activation (compare the α-OAc group in **XIII**).[47,50,51] Second, due to the electrophilicity of the hydrogen abstractor TBADT (featuring an oxygen-centered radicaloid character),[52] the deactivation exerted at C-1 by the presence of the acetoxy group may direct the selective formation of an α-oxy radical at C-5.

Indeed, when β-tetra-O-acetylfucose **1-βOAc** was treated with 1.1 equiv. of methyl acrylate **2a** in the presence of 5 mol% TBADT in CH_3CN upon 370 nm irradiation for 20 h, 55% conversion of **1-βOAc** resulted, leading to **3-βOAc** as the exclusive product (97% yield brsm; Figure 3 A). The structure of **3-βOAc** was safely assigned based on NMR

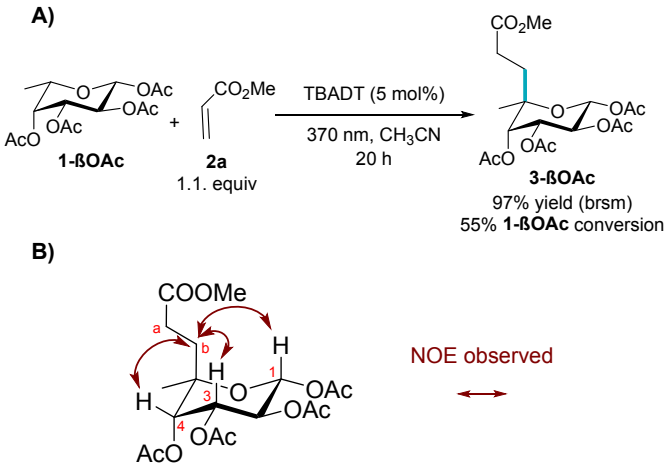

Fig. 3 A) TBADT promoted Giese-type alkylation of β-tetra-*O*-acetylfucose **1-βOAc** with methyl acrylate **2a**. Isolated yield of **3-βOAc** based on consumed **1-βOAc**; **B)** NOESY experiments allowed to establish the C-5 configuration of **3-βOAc**.

spectroscopy,showing the disappearence of the H-5 proton of fucose and the presence of a quaternary carbon at 77.3 ppm (see Supporting Information, section 2.3 for the full spectra assignment). NOESY experiments showed clear cross peaks between the axial protons on the ring (H-1 and H-3) and the protons on the newly introduced alkyl chain (Figure 3 B), while no correlation was observed between H-6 (Me) and H-1 or H-3. The NOESY crosspeak observed between fucose H-4 and the ester alkyl chain further supports the regiochemistry assignment.

Thus, the TBADT photocatalyzed alkylation of **1-βOAc** was fully regio- and stereoselective. Encouraged by these results, we moved to extend the scope of this remarkable transformation to a series of purposely prepared (see Supporting Information, section 2.3) tri-O-acetyl-β-fucosides **1-βR,** bearing different substituents at the anomeric position (Figure 4 A). For this set of experiments, all reactions were performed again in the presence of **2a** and 5 mol% TBADT, but shortening the reaction time to 7 h, since prolonged irradiation did not improve **1-βR** conversion. Starting from β-methyl fucoside (**1-βOMe**), the ester **3-βOMe** was obtained in 64% yield brsm (87% **1-βOMe** conversion), together with a by-product deriving from the incorporation of **2a** via C–H cleavage of the OMe group (10% yield brsm). Noteworthy, no alkylation of the anomeric position was observed, even upon prolonged reaction time (20 h), indicating that the presence of an acetoxy group is not mandatory to avoid the functionalization at C-1. Overall, a good conversion was observed for essentially all **1-βR** tested (Figure 4 A). The yields largely depended on the substituent at the anomeric position, which, in some cases, induced the formation of some oligomeric products (as in the case of **3-βN_3**).

The reaction was particularly effective with the 1-cyano-fucoside **1-βCN**, the phenylthio-fucoside **1-βSPh**, and 1-carbomethoxy fucoside **1-βCO_2Me**, which afforded the corresponding adducts **3-βCN**, **3-βSPh** and **3-βCO_2Me** in 90%, 70% and 80% yield, respectively. The reaction was likewise tolerant to the presence of an *N*-amide group at the anomeric position (**1-βNHCOPh**). Moreover, in the preparation

View Article Online
DOI: 10.1039/D5GC05775B

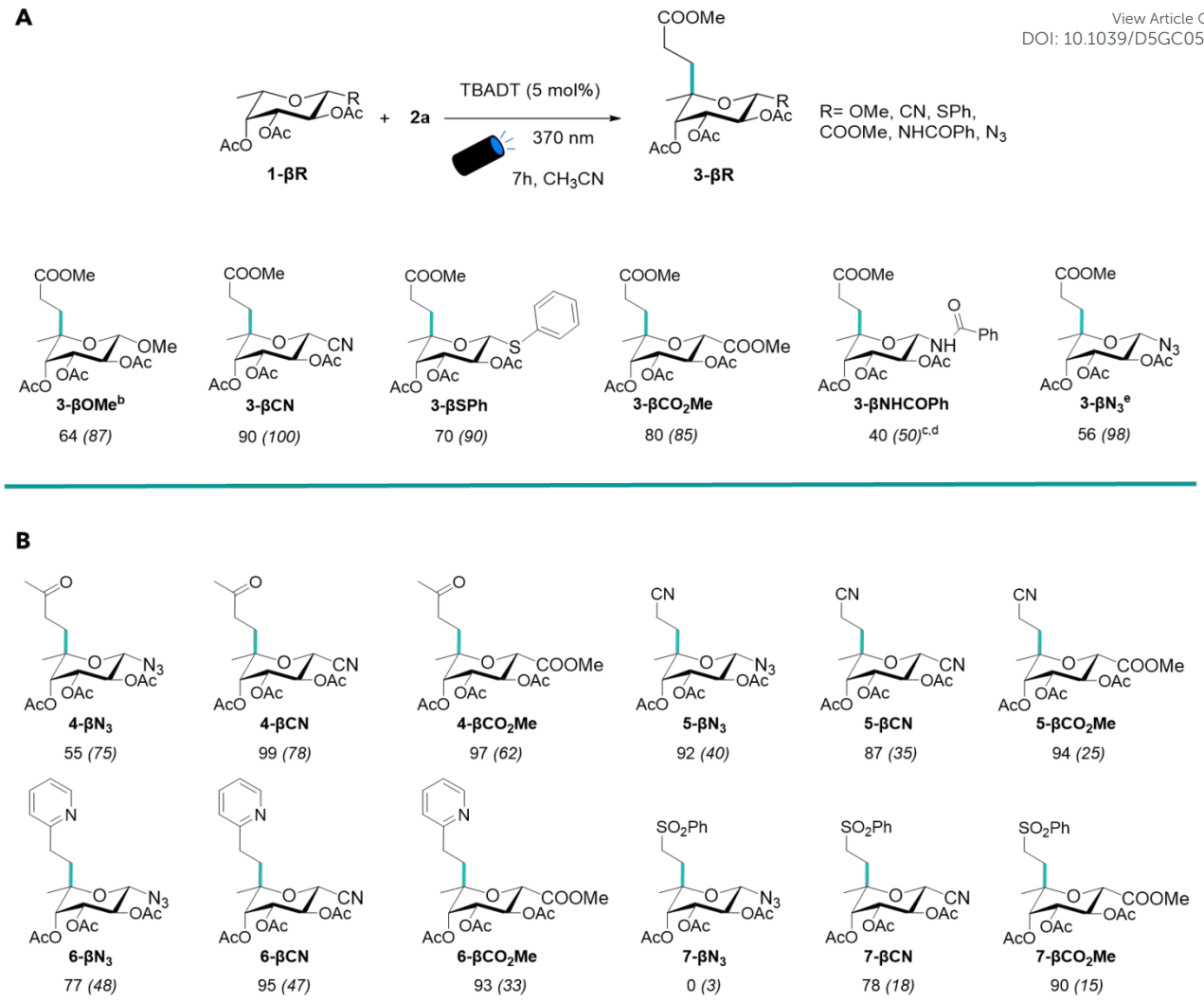

Fig. 4 Scope of: **A)** β-Fucosides and **B)** Alkenes**.** [a] Reaction conditions: **1-βR** (1 equiv, 0.1 M), methyl acrylate **2a** (1.1 equiv), TBADT (5 mol%) under 370 nm irradiation in MeCN for 7 h. The C-5 configuration of all products was established by NOESY experiments. **3-βR** Isolated yield brsm and (**1-βR** *% conversion*) are reported. Conversions were determined by ^{1}H-NMR of the crude reaction mixtures. [b] Alkylated by-product on OMe was also formed (10% yield); [c] 20 h irradiation; [d] Yields were estimated by ^{1}H-NMR analysis of the crude reaction mixture since **3-βNHCOPh** was inseparable from the remaining **1-βNHCOPh**; [e] 3 h irradiation. An oligomeric adduct was also formed in 12% yield).

of **3-βN$_3$**, the reaction time could be shortened to 3 h. In all cases, a single isomer was isolated and NMR experiments (see data in Supporting Information) evidenced that the reaction showed the same site selectivity and stereoselectivity observed for **1-βOAc**.

Further experiments to improve the conversion of **1-βR** and/or the yield of **3-βR** by varying the reaction medium, the catalyst loading, etc. were unsuccessful. However, the process did not take place in the absence of either photocatalyst or light (Table S1).

Substrates **1-βN$_3$**, **1-βCN** and **1-βCO$_2$Me** were then selected to test the alkene scope of the reaction by using methyl vinyl ketone **2b**, acrylonitrile **2c**, vinyl pyridine **2d** and phenyl vinyl sulfone **2e**, as the reaction partners (Figure 4 B). Also in this case, the reactions were consistently performed by adopting the standard conditions (5 mol% TBADT, 7 h irradiation). Notably, a fully regio- and stereoselective derivatization at C-5 was observed, as assessed by NOESY experiments (see Supporting Information). Thus, functionalization of **2b** with **1-βN$_3$**, **1-βCN** and **1-βCO$_2$Me** proceeded with conversions similar to those observed with **2a** (compounds **4** were formed in up to quantitative yield). As for **2c** and **2d**, despite the yields of compounds **5** and **6** are in the 77-95% range, the conversion of the fucoside did not exceed 50%. Further optimization was not beneficial to the reaction outcome (Table S2). Green metric parameters (PMI, E factor, AE end EcoScale; see Supporting Information, section 5) have been calculated for selected reactions. The values obtained range from good to excellent with a 100% Atom Economy.

Additional control experiments were performed to elucidate the reaction mechanism and have insights on the observed selectivity. First, to clarify the radical nature of the process we repeated selected experiments on **1-βOMe**, **1-βN$_3$**, **1-βCN** and **1-βCO$_2$Me** in the presence of 2 equiv. of TEMPO under otherwise standard conditions (Michael acceptor omitted; see Scheme 1). In all cases, the corresponding C-5 adducts **8-βR** were isolated in variable yields as the only product and NMR experiments (NOESY) demonstrated that the reaction takes place in a completely regio- and stereoselective fashion.

View Article Online
DOI: 10.1039/D5GC05775F

We then tested the reactivity of the fucosides depicted in Chart 1 in the model reaction with **2a**. Noteworthy, no reaction occurred when the α-fucoside **1-αOAc** (rather than the β-anomer **1-βOAc**) was subjected to the standard photocatalytic conditions, highlighting a dramatic effect of the anomeric configuration on the reaction course. Similarly, the α-methyl fucoside 1-αOMe did not react even upon prolonged irradiation (24 h). Notably, no TEMPO adducts were formed from substrates **1-αOAc** and **1-αOMe**.

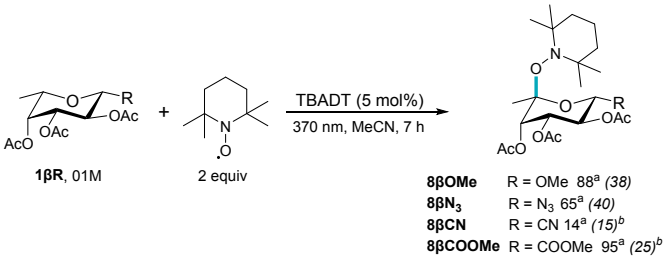

Scheme 1 Trapping Experiments with TEMPO. [a] Isolated yields (**1-βR** *% conversion*). [b] 1h irradiation.

The effect of the protecting groups on the photoreactivity of **1-βCN** was also investigated. Thus, the unprotected cyanoderivative **9** gave rise to a complex mixture of products and changing the acetoxy groups (in compound **1-βCN**) for the silyloxy (compound **10**) or benzyloxy (compound **11**) groups led again to a complex mixture of products (Chart 1). The latter experiments safely confirmed the crucial role of the OAc protecting groups in directing the process toward a selective transformation.

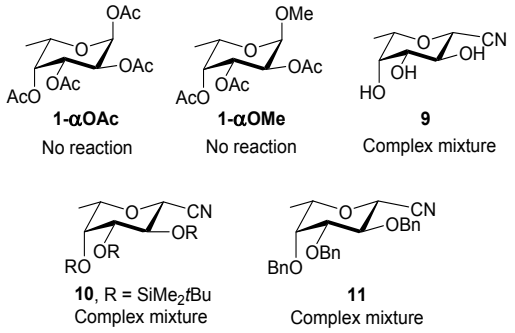

Chart 1 Control reactions on substituted fucosides (0.1 M) under TBADT photocatalyzed conditions in the presence of **2a** (1.1 equiv.).

Deuteration experiments. To have further insights into the reasons underlying the observed selectivity, compound **1-βCN** and TBADT (5 mol%) were irradiated in deuterated media, both in the absence and in the presence of **2a** (see section 4 in the Supporting Information). In the absence of **2a** adoption of a MeCN/D_2O mixture as the solvent resulted in a partial deuteration of **1-βCN**, with deuterium selectively installed at C-5, as observed by ^{1}H-NMR analysis. No deuteration took place in CD_3CN. On the other hand, the presence of **2a** (tested only in MeCN/D_2O) mainly led to monodeuterated **3-βCN-D,** where deuteration occurred in the α-position with respect to the ester moiety (^{1}H-NMR).

LFP experiments. Laser-Flash Photolysis (LFP) experiments were also conducted on selected substrates (**1-βOMe**, **1-βN$_3$**, **1-βCN** and **1-αOMe**), to investigate the kinetics of the C–H cleavage step; in particular, the quenching rates of the excited state of TBADT (labelled **wO**)[52] by the above-mentioned fucosides were measured (detailed methodologies are provided in Section 3 of the Supporting Information). For each sugar, a Stern-Volmer (SV) plot was constructed and a kinetic constant for the HAT step was calculated. SV analysis revealed, for β fucosides **βOMe**, **1-βN$_3$** and **1-βCN**, high quenching rates, resulting in kinetic constants – respectively: 4.4×10^8 $M^{-1}\cdot s^{-1}$, 6.3×10^8 $M^{-1}\cdot s^{-1}$, 4.9×10^8 $M^{-1}\cdot s^{-1}$ – comparable to those already observed for excellent hydrogen donors (e.g. isopropanol[53] or various aldehydes[54]). On the contrary, as shown in Figure 5, **1-αOMe** is characterized by a remarkably lower kinetic constant (1.4×10^7 $M^{-1}\cdot s^{-1}$), in accordance with the experimental behaviour observed for this substrate.

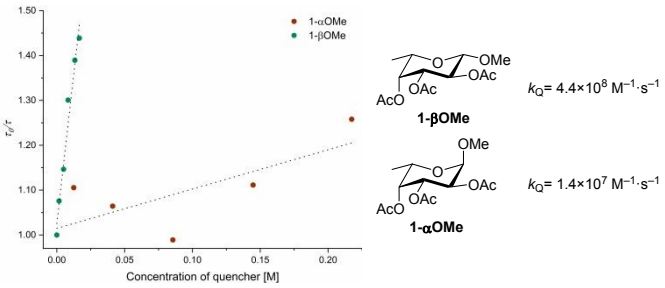

Fig. 5 Stern-Volmer plots and quenching constants for **1-βOMe** and **1-αOMe** measured at 25 °C in MeCN.

Computational investigation. To get further insight into the observed reactivity patterns, we performed computational work on reference compounds **1-βOAc** and **1-αOAc**. In particular, we determined the reaction parameters characterizing the C–H cleavage at positions C-1 and C-5 of named fucosides by the oxygen-centered radical tBuO•, a convenient prototype of a hydrogen abstractor species, mimicking the behaviour of the decatungstate reactive state.[54] To such end, we employed density functional theory at the ωB97xD/def2TZVP level of theory, with MeCN as reaction medium modeled through an implicit approach, to optimize the geometries of relevant compounds, radical intermediates and transition states (see Section 6, Supporting Information for further details). Figure 6 shows both the energy barrier ($\Delta G^‡$; solid bars) and energy change (ΔG; dashed bars) values of the modeled hydrogen atom transfer processes, offering a measure of the associated kinetic and thermodynamic parameters, respectively.

As apparent from the graph, all the studied C–H cleavage reactions are exergonic in nature, with the radical intermediates at C-5 being similarly stabilized in **1-βOAc** and **1-αOAc** (ΔG around -10 kcal·mol^{-1}), and in both cases to a larger extent than the corresponding radicals at C-1. As for the anomeric (C-1) radicals, the axial radical formed from the **β**-isomer **1-βOAc** benefits of a larger stabilization ($\Delta G \sim$ -7.8 kcal·mol^{-1}) than the equatorial one, formed from the **α**-isomer **1-αOAc** ($\Delta G \sim$ -5.0 kcal·mol^{-1}), as expected based on anomeric stabilization of the axial radical.[55,56] Thermodynamic parameters, however, merely give an indication about the feasibility of the studied processes, while kinetic parameters are typically more important to elucidate selectivity profiles. Along this line, in **1-βOAc** the C–H cleavage at C-5 ($\Delta G^‡ \sim$ +12.9 kcal·mol^{-1}) has to confront a smaller energy barrier than that at C-1 ($\Delta G^‡ \sim$ +19.6 kcal·mol^{-1}), with

a quite large $\Delta\Delta G^{‡}$ (> 6.7 kcal·mol^{-1}) that fully aligns with the observed regioselectivity. A similar situation is observed in **1-αOAc**, although the $\Delta G^{‡}$ associated with C–H cleavage at C-5 is larger (~ +13.8 kcal·mol^{-1}), while that at C-1 is smaller (~ +17.4 kcal·mol^{-1}), resulting in a reduced $\Delta\Delta G^{‡}$ (~ 3.6 kcal·mol^{-1}) for regioselectivity.

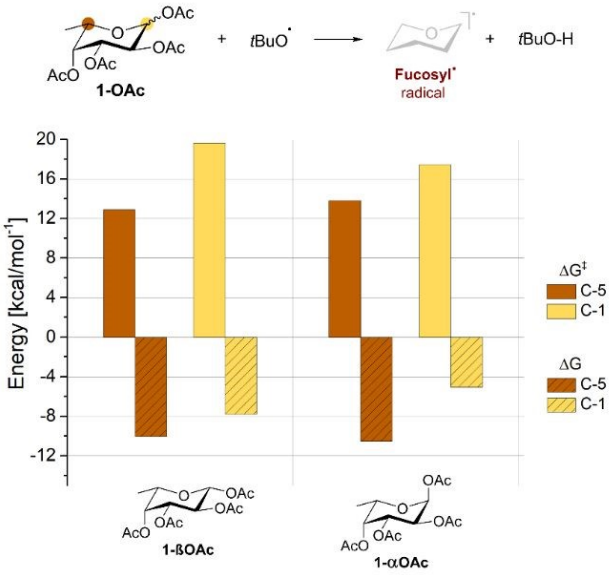

Fig. 6 Energy barrier ($\Delta G^{‡}$; solid bars) and energy change (ΔG; dashed bars) values for the modeled hydrogen atom transfer processes, as from calculations at the ωB97xD/def2TZVP level of theory in bulk acetonitrile (see Section 6, Supporting Information for additional details).

Discussion

The results reported above show that C-5 functionalization of β-fucosides can be achieved by TBADT-photocatalyzed HAT activation, in a way well beyond our initial expectations. In particular, although the reaction appears to require acetylation of positions 2-4 of the sugar, it is surprisingly tolerant of various anomeric substituents, provided that they are not in the α position (Figure 4). From a preparative point of view, it is noteworthy that excellent conversions and yields were obtained for the β-phenylthiofucoside **3-βSPh**, which in principle can be directly activated as a (C-5 modified) fucosyl donor.[57] Similarly remarkable is the reactivity of the β-fucosyl azide **1-βN$_3$**, which gave satisfactory yields of the C-5 Giese alkylation product **3-βN$_3$**, despite the known photochemical lability of alkylazides.[58] In this regard, glycosyl azides are important intermediates in the synthesis of glycosylamides and other *N*-glycosyl derivatives.[59]

On the contrary, no reaction occurred on any of the α-substrates tested (**1-αOAc** and **1-αOMe**, Chart 1). LFP experiments performed on **1-αOMe** (Figure 5) showed that this compound is kinetically inert vs the excited state of TBADT, which is consistent with the strong steric effects typically observed for the bulky decatungstate anion.[48] It is perhaps more surprising that C-5 regioselectivity persists in the reaction of the **1-βOMe** anomer, even if the anomeric position could now provide an axial radical, potentially doubly stabilized by the two acetal oxygens. Indeed, it is well-established that axial radicals in anomeric positions are both energetically favored and more nucleophilic than the equatorial counterpart, due to stereo-electronic effects.[60,61] However, it is likewise well-known that anomeric interaction effects are not additive, hence, the stabilizing effect of the second oxygen atom at C-1 should not be expected to direct the regioselectivity.[62,63] Additionally, thermodynamic stability of the radical intermediate is clearly not the determining factor in this reaction, otherwise the captodative anomeric radical at C-1 in **1-βCN** and **1-βCOOMe** would shift regioselectivity from C-5 to C-1 – which does not occur. As it happens, C-5 selectivity persists with all the β-anomeric substituents we tested, irrespective of their electronic and steric characteristics, as also supported by the TEMPO trapping experiments (Scheme 1). Thus, the observed reactivity is more consistent with kinetic control in the C–H activation step, which is also consistent with our computational studies (Figure 6). On one hand, the markedly different energy barriers for C–H cleavage determined in **1-βOAc** support the complete selectivity toward C-5 functionalization observed for such substrate. At the same time, the lack of reactivity shown by **1-αOAc** can be traced back to the less favorable C–H cleavage at C-5, possibly due to the steric hindrance exerted by the axial acetoxy group installed at C-1; such effect is expected to be even more pronounced in the case of the bulky decatungstate anion,[48,49] compared with the simplified hydrogen abstractor tBuO• employed here. In terms of energy barriers for C–H cleavage, the hereby reported values align well with those recently reported by some of us for the successful functionalization of the formyl C–H bond in α-tert-butoxy acetaldehyde ($\Delta G^{‡}$ for C–H cleavage ~ +12.1 kcal·mol^{-1}).[54]

Overall, the above considerations are consistent with a mechanism (Scheme 2) in which the excited decatungstate anion (in its reactive state **wO**) abstracts the C-5 hydrogen atom from **1-βR** under kinetic control. The resulting radical **1-βR•**, whose formation is validated by the TEMPO-trapping experiments, is stabilized in the axial position by anomeric-like interactions with the ring oxygen and stereoselectively reacts with the Michael acceptor, yielding intermediate **3-βR•**, which ultimately restores the decatungstate anion $[W_{10}O_{32}]^{4-}$ in its original state, forming Giese-type product **3-βR**. This mechanistic scenario is further corroborated by deuteration experiments. The absence of deuteration in CD_3CN rules out hydrogen atom abstraction from the solvent, while the partial deuteration patterns observed in the presence of D_2O are compatible with H/D scrambling at the reduced photocatalyst stage ($H^+[W_{10}O_{32}]^{5-} \rightleftarrows D^+[W_{10}O_{32}]^{5-}$) followed by back-H (or D) donation to **1-βR•** or **3-βR•** (in the presence of **2a**).[64]

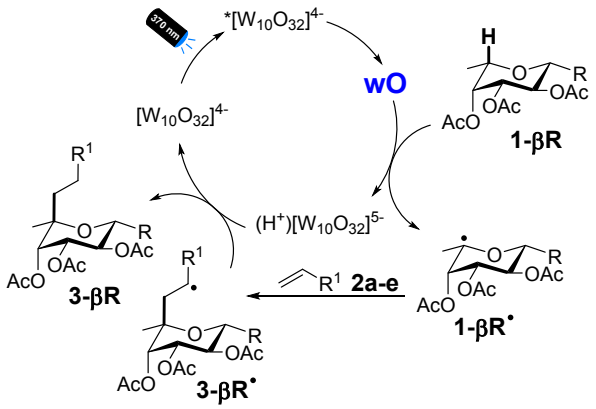

Scheme 2 Mechanistic proposal.

Conclusions

In this paper, we showed the development of an efficient green methodology for the site-selective and stereoselective alkylation of position 5 in β-fucosides by means of decatungstate photocatalyzed Giese-type alkylation. This photocatalyst may be easily prepared in a one-step procedure starting from inexpensive starting materials.[65] Mechanistic studies supported that kinetic effects are likely to determine the C-5 regioselectivity for the TBADT-mediated hydrogen atom abstraction, which enables the overall transformation. The exclusive axial selectivity of the alkylation is attributed to stabilizing interactions of the axial C-5 radical with the ring oxygen, which parallel those well-established for anomeric (C-1) radicals. The reaction is efficient, versatile and tolerant of various Michael acceptors and anomeric substituents on the fucose ring, including C-, N- and S-glycosides.

The totally unprecedented reactivity we described here for the easy access to a range of C-5 alkylated fucosides via late stage functionalization of β-fucosides has a number of potential applications in the synthesis of fucose-based glycomimetics. L-fucose is a widespread component of mammalian glycans, where it plays essential functions in cell regulation and immune homeostasis. Abnormal fucosylation is one of the hallmarks of cancer and can be therapeutically targeted. Thus, expanding the chemical space available to fucose-based ligands and inhibitors is a major contribution to the glycotool-box. The chemical reactivity and 3D conformational properties of this new class of C-5 modified fucose rings will need to be established, as well as the potential extension of the present transformation to different monosaccharides. Studies are in progress in our laboratories along these lines.

Author contributions

S. M., M. F. and A. B. conceived and supervised the research. E. C., M. P., D. R. and M. G. designed and performed the experiments. S. M., M. F., D. R. and A. B. analysed the data and wrote the manuscript. All authors discussed the results and commented on the manuscript

Conflicts of interest

"There are no conflicts to declare".

Data availability

View Article Online
DOI: 10.1039/D5GC05775B

The data supporting this article have been included as part of the ESI.†

Acknowledgements

The project is supported by EU funding within the NextGeneration EU-MUR PNRR Extended Partnership initiative on Emerging Infectious Diseases (Project no. PE00000007, INF-ACT) and, in part, within the GREEN TECH project of Regione Lombardia (Bando collabora e Innova) and the MUSA–Multilayered Urban Sustainability Action–project, funded by the European Union–NextGenerationEU under the National Recovery and Resilience Plan (NRRP) Mission 4 Component 2 Investment Line 1.5: Strengthening of research structures and creation of R&D "innovation ecosystems", set up of "territorial leaders in R&D". HMRS Mass spectrometry analyses were performed at the Mass Spectrometry facility of the Unitech COSPECT at Università degli Studi di Milano. The authors acknowledge the CINECA award under the ISCRA initiative, for the availability of high-performance computing resources and support. Support from the Ministero dell'Università e della Ricerca (MUR) and the University of Pavia through the program "Dipartimenti di Eccellenza 2023–2027" is gratefully acknowledged.

M.F. thanks the financial support provided by the Project PRIN PNRR 'LIGHT CAT' (no. P2022RHMCM) supported by the European Commission – NextGeneration EU programme.

Notes and references

1 C. T. Campbell, S.-G. Sampathkumar and K. J. Yarema, *Mol. Biosyst.*, 2007, **3**, 187-194.
2 N. Probst, G. Grelier, S. Dahaoui, M. Alami, V. Gandon and S. Messaoudi, *ACS Catal.*, 2018, **8**, 7781–7786.
3 J. Ghouilem, C. Tran, N. Grimblat, P. Retailleau, M. Alami, V. Gandon and S. Messaoudi, *ACS Catal.*, 2021, **11**, 1818–1826.
4 J. Wu, A. Kopp and L. Ackermann, *Angew. Chem. Int. Ed.*, 2022, **61**, e202114993.
5 C. S. Bennet, *Selective Glycosylations: Synthetic Methods and Catalysts*, Wiley, 2017.
6 R. Das and B. Mukhopadhyay, *ChemistryOpen*, 2016, **5**, 401–433.
7 S. Vidal, Analysis and preparation of Glycans. In *Comprensive Glycoscience*, J. J. Jr. Barchi Ed., Elsevier, 2021.
8 Y. Jiang, Y. Zhang, B. C. Lee and M. J. Koh, *Angew. Chem. Int. Ed.*, 2023, **62**, e202305138.
9 D. J. Gorelik, S. P. Desai, S. Jdanova, J. A. Turner and M. S. Taylor, *Chem. Sci.*, 2024, **15**, 1204–1236.
10 H. Xie, S. Wang and X.-Z. Shu, *J. Am. Chem. Soc.*, 2024, **146**, 32269–32275.
11 S. Dubey, Z. Azeem and P. K. Mandal *Adv. Synth. Catal.*, 2024, **366**, 4017–4041.
12 J. Wang, F. Zhou, Y. Xu and L. Zhang, *Chem. Asian J.*, 2025, **20**, e202401114.

13 Y. Jiang, Y. Wei, Q. Y. Zhou, G. Q. Sun, X. P. Fu, N. Levin, Y. Zhang, W. Q. Liu, N. X. Song, S. Mohammed, B. G. Davis and M. J. Koh, *Nature*, 2024, **631**, 319–327.
14 V. Dimakos and M. S. Taylor, *Chem. Rev.*, 2018, **118**, 11457–11517.
15 T. G. Frihed, M. Bols and C. M. Pedersen, *Eur. J. Org. Chem.*, 2016, **2016**, 2740–2756.
16 A. Shatskiy, E. V. Stepanova and M. D. Kärkäs, *Nat. Rev. Chem.*, 2022, **6**, 782–805.
17 C. C. J. Loh, *Chem. Catal.*, 2024, **4**, 100891.
18 L. Xia, Q. Huang and L. Dai, *Org. Chem. Front.*, 2024, **11**, 4926–4933.
19 C. E. Suh, H. M. Carder and A. E. Wendlandt, *ACS Chem Biol.,* 2021*,* **16***,* 1814-1828*.*
20 A. Tamburrini, C. Colombo and A. Bernardi, *Med. Res.,* 2020, **40**, 495–531.
21 A. Bernardi and S. Sattin, *Eur. J. Org. Chem.*, 2020, **2020**, 4652–4663.
22 L. Capaldo, D. Ravelli and M. Fagnoni, *Chem. Rev.*, 2022, **122**, 1875–1924.
23 J. N. Capilato, C. R. Pitts, R. Rowshanpour, T. Dudding and T. Lectka, *J. Org. Chem.*, 2020, **85**, 2855–2864.
24 Y. Li and Y. Kuninobu, *Adv. Synth. Catal.*, 2023, **365**, 2577–2587.
25 E. Kurokawa, Y. Li, S. Okuyama, K. Sekine and Y. Kuninobu, *J. Org. Chem.*, 2025, **90**, 7801–7808.
26 J. L. Jeffrey, J. A. Terrett and D. W. C. MacMillan, *Science*, 2015, **349**, 1532–1536.
27 I. C. Wan, M. D. Witte and A. J. Minnaard, *Chem. Commun.*, 2017, **53**, 4926–4929.
28 A. Matsumoto, M. Yamamoto and K. Maruoka, *ACS Catal.*, 2022, **12**, 2045–2051.
29 M. L. M. C. Mouthaan, K. Pouwer, M. L. G. Borst, M. D. Witte and A. J. Minnaard, *Synthesis*, 2022, **54**, 4683–4689.
30 Y.-A. Zhang, X. Gu and A. E. Wendlandt, *J. Am. Chem. Soc.*, 2022, **144**, 599–605.
31 Y. Wang, H. M. Carder and A. E. Wendlandt, *Nature*, 2020, **578**, 403–408.
32 C. J. Oswood and D. W. C. MacMillan, *J. Am. Chem. Soc.*, 2022, **144**, 93–98.
33 H. M. Carder, Y. Wang and A. E. Wendlandt, *J. Am. Chem. Soc.*, 2022, **144**, 11870–11877.
34 H. M. Carder, G. Occhialini, G. Bistoni, C. Riplinger, E. E. Kwan and A. E. Wendlandt, *Science*, 2024, **385**, 456–463.
35 Y. Masuda, H. Tsuda and M. Murakami, *Angew. Chem. Int. Ed.*, 2020, **59**, 2755–2759.
36 S. Xu, Y. Ping, M. Xu, G. Wu, Y. Ke, R. Miao, X. Qi and W. Kong, *Nat. Chem.*, 2024, **16**, 2054–2065.
37 L. Somsák and K. Czifrák, Radical-mediated Brominations at Ring-positions of Carbohydrates – 35 Years Later. In *Advances in Carbohydrate Chemistry and Biochemistry*, ed. A. L. T. Pilar Rauter, The Royal Society of Chemistry, 2013, vol. 39, pp. 1–37.
38 S. Mazzotta, J. Gori, G. Cavazzoli, S. Sattin, G. Macetti and A. Bernardi, *Eur. J. Org. Chem.,* 2025*,* **28***,* e202500599.
39 J. D. McCarter and S. G. Withers, *J. Am. Chem. Soc.*, 1996, **118**, 241–242.
40 X. Cao, X. Du, H. Jiao, Q. An, R. Chen, P. Fang, J. Wang and B. Yu, *Acta Pharm. Sin. B*, 2022, **12**, 3783–3821.
41 R. Bermeo, K. Lal, D. Ruggeri, D. Lanaro, S. Mazzotta, F. Vasile, A. Imberty, L. Belvisi, A. Varrot and A. Bernardi, *ACS Chem. Biol.*, 2022, **17**, 2899–2910.
42 S. Mazzotta, G. Antonini, F. Vasile, E. Gillon, J. Lundstrøm, A. Varrot, L. Belvisi and A. Bernardi, *Molecules*, 2023, **28**, 1494.
43 G. Antonini, A. Bernardi, E. Gillon, A. Dal Corso, M. Civera, L. Belvisi, A. Varrot and S. Mazzotta, *J. Med. Chem.*, 2024, **67**, 19546–19560.
44 G. Antonini, M. Fares, D. Hauck, P. Mała, E. Gillon, L. Belvisi, A. Bernardi, A. Titz, A. Varrot and S. Mazzotta, *J. Med. Chem.*, 2025, **68**, 9681–9693.
45 H. M. Flowers, in *Adv. Carbohydr. Chem.*, 1981, **39**, 279–345.
46 V. Dimakos, H. Y. Su, G. E. Garrett and M. S. Taylor, *J. Am. Chem. Soc.*, 2019, **141**, 5149–5153.
47 G. Zhang, N. W. See, N. Wimmer, M. J. Godinez, S. A. Cameron, R. H. Furneaux and V. Ferro, *Org. Lett.*, 2024, **26**, 5956-5960.
48 a) D. Ravelli, M. Fagnoni, T. Fukuyama, T. Nishikawa and I. Ryu, *ACS Catal.*, 2018, **8**, 701–713. b) K. Yamada, T. Fukuyama, S. Fujii, D. Ravelli, M. Fagnoni and I. Ryu, *Chem. Eur. J.,* 2017, **23**, 8615–8618.
49 D. Ravelli, S. Protti and M. Fagnoni, *Acc. Chem. Res.*, 2016, **49**, 2232–2242.
50 J. Hammoud, A. Joosten and T. Lecourt, *Carbohydr. Res.,* 2019*,* **486***,* 107834.
51 M. Boultadakis-Arapinis, V. Gandon, E. Prost, L. Micouin and T. Lecourt, *Adv. Synth. Catal.*, 2014, **356**, 2493–2505.
52 V. De Waele, O. Poizat, M. Fagnoni, A. Bagno and D. Ravelli, *ACS Catal.*, 2016, **6**, 7174–7182.
53 D. Dondi, M. Fagnoni and A. Albini, *Chem. Eur. J.*, 2006, **12**, 4153–4163.
54 E. Cassera, V. Martini, V. Morlacci, S. Abrami, N. Della Ca', D. Ravelli, M. Fagnoni and L. Capaldo, *JACS Au*, 2025, **5**, 3491-3499.
55 B. Giese and J. Dupuis, *Angew. Chem. Int. Ed.*, 1983, **22**, 622–623.
56 H. Abe, S. Shuto and A. Matsuda, *J. Am. Chem. Soc.*, 2001, **123**, 11870–11882.
57 J. D. C. Codée, R. E. J. N. Litjens, L. J. van den Bos, H. S. Overkleeft and G. A. van der Marel, *Chem. Soc. Rev.*, 2005, **34**, 769–782.
58 N. Gritsan and M. Platz, in *Organic Azides*, eds. S. Bräse and K. Bakert, Wiley, 2009, pp. 311–372.
59 Z. Györgydeák and J. Thiem, in *Advances in Carbohydrate Chemistry and Biochemistry*, Elsevier, 2006, pp 103-182.
60 B. Giese, *Angew. Chem. Int. Ed.*, 1989, **28**, 969–980.
61 I. V. Alabugin, L. Kuhn, M. G. Medvedev, N. V. Krivoshchapov, V. A. Vil', I. A. Yaremenko, P. Mehaffy, M. Yarie, A. O. Terent'ev and M. A. Zolfigol, *Chem. Soc. Rev.*, 2021, **50**, 10253–10345.
62 A. S. Menon, D. J. Henry, T. Bally and L. Radom, *Org. Biomol. Chem.*, 2011, **9**, 3636–3657.
63 Y.-R. Luo, *Handbook of Bond Dissociation Energies in Organic Compounds*, Taylor & Francis, 2002.
64. I. Ryu, A. Tani, T. Fukuyama, D. Ravelli, M. Fagnoni and A. Albini *Angew. Chem. Int. Ed.* 2011, **50**, 1869–1872.
65 S. Protti, D. Ravelli, M. Fagnoni and A. Albini, *Chem. Commun.*, 2009, **47**, 7351–7353.

View Article Online
DOI: 10.1039/D5GC05775B

Data Availability Statement

- The data supporting this article have been included as part of the ESI.†